Post-fault oscillation phenomenon in compensated MV-networks challenges earth-fault protection

Ari WAHLROOS, Janne ALTONEN
ABB Oy Medium Voltage Products – Finland
ari.wahlroos@fi.abb.com, janne.altonen@fi.abb.com

Hanna-Mari PEKKALA
Elenia Oy – Finland
hanna-mari.pekkala@elenia.fi

ABSTRACT

One of the special challenges for earth-fault protection in compensated MV-networks is the post-fault oscillation, which is initiated as the fault is cleared by tripping or by self-extinguishment of the fault arc. During this transient process the network returns back to the healthy state through oscillations with frequency and time constant defined by network parameters. In case of permanent fault such oscillation is experienced only momentarily, but during intermittent earth fault the oscillation repeats itself between fault pulses. Due to decaying nature and possible off-nominal frequency of the oscillation, false operations of earth-fault protection may occur. This is especially valid in networks with distributed compensation where the central coil is not used or it is temporarily disconnected. In this paper, first the theory of post-fault oscillation is presented with a simple equivalent circuit. Secondly a hand calculation procedure is suggested for evaluating the risk of false operation of basic earth-fault protection due to transient overcompensation of the protected feeder caused by post-fault oscillation. Primary earth-fault tests conducted in a practical distribution network verify the correctness and effectiveness of the procedure. It is also shown that the neutral admittance based earth-fault protection provides enhanced stability during post-fault oscillations without endangering high sensitivity of protection.

BACKGROUND OF THE STUDY

A transient phenomenon that resulted in maloperation of earth-fault protection is described in [1]: There had been unexplainable relay protection failures in one substation during earth faults. The network was operated with only distributed compensation coils, and when an earth fault occurred in one of the feeders, the faulted feeder was correctly disconnected. But during the post-fault oscillations, a cable feeder with one distributed coil connected to it was wrongly disconnected from the substation although there was no fault in it. The maloperation had happened several times.

Similar protection maloperation was later repeated in the joint field test conducted in October 2013 by ABB Oy and utility Elenia Oy in the Vilppula Substation, ***Fig. 1***. The total uncompensated earth-fault current of the substation is 196A. Six distributed coils in the network suppress 80A of the total capacitive earth-fault current. The rest is compensated by the central coil. Total resistive shunt losses of the system are ~4A and the parallel resistor of the central coil produces additional ~5A. In these tests, special attention was paid on the behavior of the feeder *J05*, which is a long cable feeder with uncompensated earth-fault current of 86A and three distributed coils (15A each) connected along it. In order to compare the performance of different earth-fault protection functions, *residual current* and *admittance based* functions were used in parallel as the basic directional earth-fault protection.

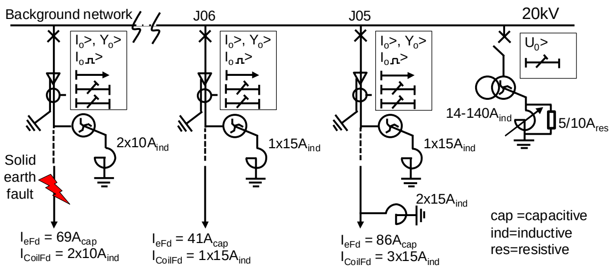

Fig.1 *Simplified single line diagram of the Vilppula substation. Background network is represented with a single equivalent feeder.*

When a trial earth fault was conducted outside feeder *J05*, while the central coil was temporarily disconnected, the basic protection functions of all healthy feeders operated correctly during the fault (no start, no operate). But during long lasting post-fault oscillations, the basic protection functions of the healthy feeder *J05* operated falsely. However, in the other healthy feeders, such as *J06*, no false operations were obtained. False operations were neither obtained with the central coil connected.

The operating point trajectories of the basic protection for the feeders *J05* and *J06* during an outside earth fault and during post-fault oscillation are shown in ***Fig. 2***.

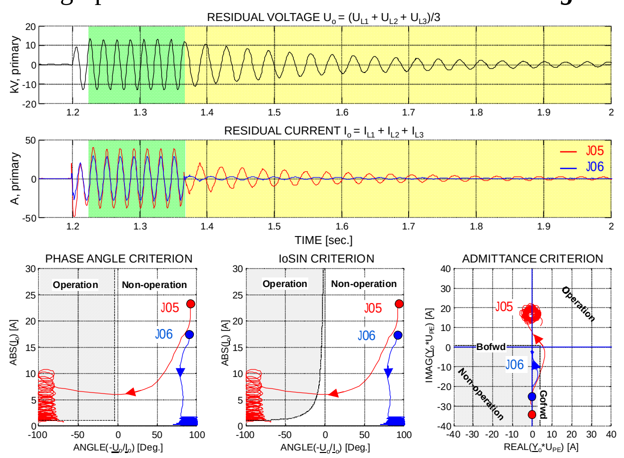

Fig. 2 *Protection operation point trajectories for the feeders J05 (red) and J06 (blue) during an outside earth fault and during post-fault oscillation. For the admittance protection, conversion to current is used,* $\underline{I}_o' = \underline{Y}_o * U_{PE}$.

During the fault (time interval marked with green color) the residual currents of the feeders *J05* and *J06* are in phase and capacitive, thus the fault is correctly seen as being outside the protected feeder. However, during the post-fault oscillation (time interval marked with yellow color), the residual currents of *J05* and *J06* are in phase opposition, *J06* is still capacitive, but *J05* is temporarily inductive. Thus the protection of the feeder *J05* sees this condition falsely as the fault being inside the protected feeder.

This paper explains the root cause and the theory of the described maloperation. Additionally means to prevent such maloperation by relay settings are presented in order to maintain high security and dependability of protection.

THEORY

A single-phase RLC-equivalent circuit of a compensated MV-network shown in ***Fig. 3*** is used to analyse the post-fault oscillation. The fault resistance and the natural asymmetry of the network are neglected in the study. It has also been assumed that the oscillation is initiated by a temporary transient fault, thus the connection status of the network is not changed due to the fault.

With the switch *SW1* closed a steady state earth fault outside the protected feeder can be analysed. When the switch *SW1* is opened at zero-crossing of the earth-fault current i_e, the post-fault oscillation is initiated. Although ***Fig. 3*** presents an outside fault, the equivalent circuit is also valid for the faulty feeder after fault current interruption, or between the fault pulses during an intermittent earth fault.

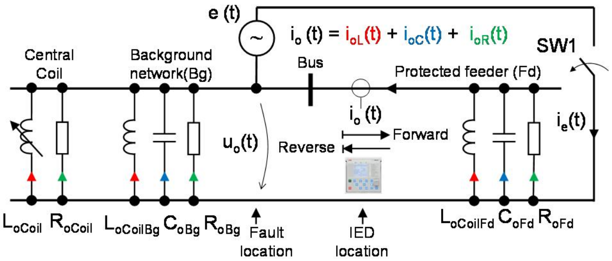

Fig. 3 *Single-phase RLC-equivalent circuit of a compensated network during an outside fault (SW1 closed) and during post-fault oscillation, which is initiated after fault current interruption (SW1 opened).*

The inductances *(L_o)*, capacitances *(C_o)* and resistances *(R_o)* of the equivalent circuit represent zero-sequence quantities, which can be calculated in primary level based on the network parameters from the utility Distribution Management System (DMS):

$L_{oCoil} = U_{PE}/(\omega_n \cdot I_{Coil})$, $R_{oCoil} = U_{PE}/(I_{Coil}/rx_{Coil} + I_{rCoil})$,

$L_{oCoilBg} = U_{PE}/(\omega_n \cdot I_{CoilBg})$, $C_{oBg} = (I_{eTot} - I_{eFd})/(\omega_n \cdot U_{PE})$,

$R_{oBg} = U_{PE}/((I_{eTot} - I_{eFd})/rx_{Net} + I_{CoilBg}/rx_{CoilDst})$,

$L_{oCoilFd} = U_{PE}/(\omega_n \cdot I_{CoilFd})$, $C_{oFd} = I_{eFd}/(\omega_n \cdot U_{PE})$,

$R_{oFd} = U_{PE}/(I_{eFd}/rx_{Net} + I_{CoilFd}/rx_{CoilDst})$, where

U_{PE} = Operating phase-to-earth voltage, w_n = Nominal angular frequency, I_{Coil} = Current of the central compensation coil, rx_{Coil} = ratio of shunt resistance and reactance of the central compensation coil, I_{rCoil} = Current of the parallel resistor of the central compensation coil, I_{CoilBg} = Total current of the distributed compensation coils located at the parallel feeders (background network), I_{eTot} = Total uncompensated capacitive earth-fault current of the network, I_{eFd} = Uncompensated capacitive earth-fault current of the protected feeder, rx_{Net} = ratio of shunt resistance and reactance of the feeders, $rx_{CoilDst}$ = ratio of shunt resistance and reactance of the distributed compensation coils, I_{CoilFd} = Total inductive current of the distributed compensation coils located at the protected feeder.

During a steady state earth fault outside the protected feeder the switch *SW1* is closed and the following time-domain equation for the residual voltage is valid [2]:

$$u_o(t) = -\sqrt{2} \cdot U_{PE} \cdot \cos(\omega_n \cdot t)$$

Post-fault oscillation is initiated as the fault becomes self-extinguished by opening the switch *SW1* at zero-crossing of the fault current. At this moment of time the phase angle difference between the residual voltage and fault current equals φ_F. For the residual voltage during the post-fault oscillation can be written:

$$u_o(t) = -\sqrt{2} \cdot U_{PE} \cdot \cos(2\pi \cdot f_P \cdot t - \varphi_P) \cdot e^{-t/\tau_P} \quad (1)$$

where

$$f_P = f_n \cdot \sqrt{I_{CoilTot}/I_{eTot} - I_{RoTot}^2/(4 \cdot I_{eTot}^2)} \quad (2)$$

$$\tau_P = 2 \cdot I_{eTot}/(\omega_n \cdot I_{RoTot}) \quad (3)$$

$$\varphi_P = \varphi_F + \pi/2, \; \varphi_F = a\tan((I_{eTot} - I_{CoilTot})/I_{R_{oTot}})$$

With the following notations:

f_P = Post-fault oscillation frequency, φ_P = Phase angle of healthy phase-to-earth voltage at the time of fault current interruption, φ_F = Phase angle difference between residual voltage and earth-fault current at the time of fault current interruption, $I_{CoilTot}$= Total inductive current of the coils in the network taking into account the central coil and the distributed coils= $I_{Coil}+I_{CoilFd}+I_{CoilBg}$, τ_P = Time constant of the post-fault oscillation, I_{RoTot} = Total resistive leakage loss current of the network = $U_{PE}/(R_{oCoil} \times R_{oFd} \times R_{oBg})/(R_{oCoil} \times R_{oBg} + R_{oCoil} \times R_{oFd} + R_{oFd} \times R_{oBg})$.

According to ***Fig. 3*** the residual current is the sum of resistive (i_{oR}), capacitive (i_{oC}) and inductive (i_{oL}) components. As post-fault oscillation can occur with off-nominal frequency, it is essential to recall the frequency dependence of the capacitive and inductive components. With decreasing frequency, the inductive current increases and capacitive current decreases proportionally to this frequency:

$i_{oC}\,[@f_P] = (f_P / f_n) \times i_{oC}\,[@f_n]$,
$i_{oL}\,[@f_P] = (f_n / f_P) \times i_{oL}\,[@f_n]$

Using the above equivalent circuit and equations, the residual voltage and residual current of the healthy feeder *J05* during steady state outside fault and during post-fault oscillation are simulated and presented in ***Fig. 4***. The post-fault oscillation is initiated at *t=0sec*. Healthy state phase-to-earth voltage is drawn as reference in the uppermost subplot. The network and feeder parameters match the Vilppula substation and feeder *J05* data described in ***Fig. 1***: U_{PE}=11.9kV, w_n=2p×50Hz, I_{eTot}=196A_{cap}, I_{Coil}=0A_{ind} (only distributed compensation applied), I_{CoilBg}=35A_{ind}, I_{CoilFd}=45A_{ind}, I_{eFd} =86A_{cap}, I_{RoTot} =3.9A_{res}. The above network and feeder parameters result in post-fault oscillation frequency of 31.9Hz and time constant of 318msec. This matches the values obtained from the actual fault recording shown in ***Fig. 2***. The phase angles and directions of the residual current components during fault and post-fault oscillation concluded from ***Fig. 4*** are listed in ***Table 1***.

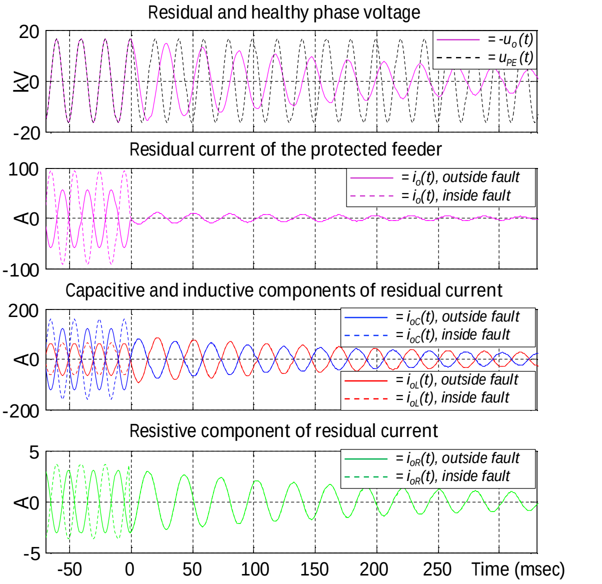

Fig. 4 *Fault quantities during steady-state fault and during post-fault oscillation. Fault current is interrupted at t=0sec.*

It can be seen that the measured residual current during post-fault oscillation in this case is seen similarly as during an inside fault. This is due to the fact that as the post-fault oscillation frequency is well below nominal the inductive residual current component is temporarily greater than the capacitive one. This leads to *transient overcompensation* of the feeder *J05*, which is the root cause of the described protection maloperation. Additional challenge for the basic directional earth-fault protection is the decaying nature and off-nominal frequency of the oscillation, which deteriorates the accuracy of phasor calculation.

Table 1. Phase angle differences and directions of the residual current components with $-u_o$ as reference.

Fault condition	*Cap. comp.* i_{oC}		*Ind. comp.* i_{oL}		*Res. comp.* i_{oR}		*Reactive comp.* $i_{oC}+i_{oL}$	
	ph.dif	dir.	ph.dif	dir.	ph.dif	dir.	ph.dif	dir.
Outside	+90°	To bus	-90°	To bus	+180°	To bus	+90°	To bus
Inside	-90°	To line	+90°	To line	0°	To line	-90°	To line
Post-fault	+90°	To bus	-90°	To bus	+180°	To bus	-90°	To bus

HAND CALCULATION PROCEDURE

Next a hand calculation procedure is presented to evaluate the risk of false operation of basic earth-fault protection due to transient overcompensation of the protected feeder caused by post-fault oscillation. This evaluation should be conducted for all feeders with distributed compensation coils.

Step 1: Determine the frequency of the post-fault oscillation f_P using ***Eq. 2***. This value is network specific i.e. determined by the parameters of the total network. Graphical presentation of ***Eq. 2*** is shown in ***Fig. 5***, which is obtained by solving the required total inductive current of the coils in the network so that a certain post-fault oscillation frequency is achieved:

$$I_{CoilTot} = (f_P / f_n)^2 \cdot I_{eTot} + 0.25 \cdot I_{RoTot}^2 / I_{eTot} \qquad (4)$$

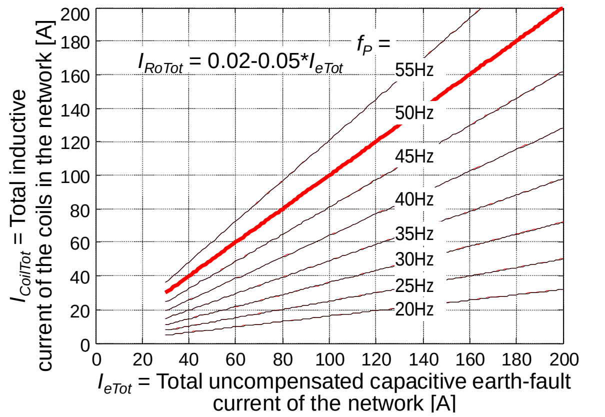

Fig. 5 *Estimate of the post-fault oscillation frequency with the given total inductive and capacitive earth-fault currents of the network.*

From ***Fig. 5*** it can be concluded that the lower the total inductive current of the coils in the network is, the lower the post-fault oscillation frequency becomes. For example, if I_{eTot}=160A_{cap} and $I_{CoilTot}$=80A_{ind}, the post-fault oscillation frequency is ~35Hz, and with lower total coil current values the oscillation frequency further decreases.

Step 2: Determine whether the residual current measured at the beginning of the protected feeder is capacitive (normal case) or if it becomes temporarily inductive (abnormal case) at the post-fault oscillation frequency f_P. This evaluation is feeder specific i.e. determined by the parameters of the protected feeder. For the evaluation, it is useful to define the *feeder compensation degree* at the post-fault oscillation frequency as $K_{Fd}[@f_P]=I_{CoilFd}[@f_P] / I_{eFd}[@f_P]$ calculated from:

$$K_{Fd}[@f_P]=(f_n / f_P)^2 \times I_{CoilFd} / I_{eFd} \qquad (5)$$

In case $K_{Fd}\ [@f_P] \geq 1.0$, the feeder becomes temporarily overcompensated due to the fact that at this frequency the coils located along the protected feeder produce more inductive current than the phase-to-earth capacitances produce capacitive current. This means that the residual current measured at the beginning of the protected feeder becomes inductive. As a result the basic protection may operate falsely, if this condition is not taken into account in settings. From ***Eq. 5*** it is also possible to solve the feeder specific *critical post-fault oscillation frequency* below which the feeder becomes temporarily overcompensated:

$$f_{PcrFd} \leq f_n \cdot \sqrt{I_{eFd} \cdot I_{CoilFd}} / I_{eFd} \qquad (6)$$

If the post-fault oscillation frequency f_P calculated in ***Step 1*** is lower than the estimated critical frequency for a given feeder, transient overcompensation of the feeder occurs during post-fault oscillation. Using ***Eq. 6*** the curves of ***Fig. 6*** can be constructed to estimate this critical frequency as a function of the total uncompensated capacitive earth-fault current of the feeder, the total inductive current of the distributed compensation coils located at the protected feeder as parameter. For example, if I_{eFd}=50A_{cap} and I_{CoilFd}=25A_{ind}, the critical frequency is ~35Hz. If the post-fault oscillation frequency calculated in ***Step 1*** is lower than (or close to) this, transient overcompensation and risk of protection maloperation exists. Duration of this condition is defined by the time constant tau, ***Eq. 3***.

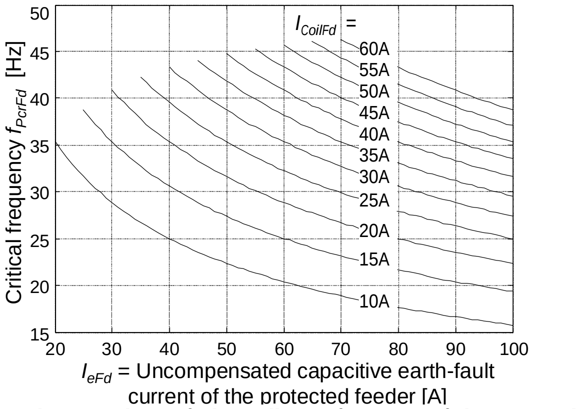

Fig. 6 *The critical post-fault oscillation frequency of the protected feeder, which results in transient overcompensation as a function of I_{eFd}, I_{CoilFd} as a parameter.*

Example – hand calculation procedure

The hand calculation procedure is used to evaluate the risk of false operation of basic earth-fault protection for the feeder *J05* at Vilppula substation. The required parameters and studied compensation degrees are listed in ***Table 2***, which also shows the calculated post-fault oscillation and critical frequencies according to ***Steps 1-2***.

Table 2. *Calculation of post-fault oscillation and critical frequencies.* $I_{eTot}=196A_{cap}$, $I_{eFd}=86A_{cap}$, $I_{coilFd}=45A_{ind}$, $I_{CoilFd}+I_{CoilBg}=80A_{ind}$

Compensation degree	I_{Coil} [A]	$I_{CoilTot}$ [A]	I_{RoTot} [A]	τ_P [ms]	f_P [Hz]	f_{PcrFd} [Hz]	$f_P < f_{PcrFd}$
Resonance	116	196	7.8	159	50.0	36.2	No
+25A	131	221	7.8	159	53.1	36.2	No
-25A	101	171	7.8	159	46.7	36.2	No
Distr. coils	-	80	3.9	318	31.9	36.2	Yes

The results of ***Table 2*** show that in case the central compensation coil is switched on, the post-fault oscillation frequency is between 46.7-53.1Hz which is clearly higher than the critical frequency of 36.2Hz for the feeder *J05*. Therefore, this feeder remains under-compensated during post-fault oscillations. However, if the central compensation coil is switched off, the post-fault oscillation frequency drops to 31.9Hz, which is well below the critical frequency. At this frequency the three distributed compensation coils produce excessive amount of inductive earth-fault current compared to the capacitive earth-fault current. This means that during the post-fault oscillation the total residual current measured at the beginning of the feeder *J05* becomes temporarily inductive. Such condition verifies the root cause of the protection maloperation in the conducted field tests and in the incident described in reference [1].

MANAGING POST-FAULT OSCILLATIONS

If a protection problem is identified based on the hand calculation procedure, settings and configuration of the protection should be verified. This is especially valid for feeders with distributed compensation coils, where earth-fault protection is based on the same functionality and settings that are applied in unearthed networks.

Neutral admittance based earth-fault protection

In case the neutral admittance based earth-fault protection is applied, the settings can be easily co-ordinated with the post-fault oscillations in the admittance plane. The equivalent residual current corresponding to the measured neutral admittance at the post-fault oscillation frequency for a healthy feeder during an outside fault equals:

$$\underline{I}'_{oP} = \underline{Y}_o \times U_{PE} = I_{RoFd} + j \times (f_n / f_P \times I_{CoilFd} \quad f_P / f_n \times I_{eFd}) \quad (7)$$

where

$\underline{Y}_o$= Measured neutral admittance, I_{RoFd} = Total leakage loss current of the protected feeder: sum of losses of the feeder and the connected distributed compensation coils = U_{PE}/R_{oFd}.

According to Vilppula substation data for the feeder *J05* ($I_{RoFd} = 2A_{res}$, f_P=31.9Hz, $I_{eFd}=86A_{cap}$, $I_{CoilFd}=45A_{ind}$), the estimated equivalent residual current during post-fault oscillation is $\underline{I}'_{oP}$ = -2.0 + j·15.7A, marked with black dot in ***Fig. 7***. This matches well with the field test measurement presented in ***Fig. 7*** (red trajectory). By setting the forward susceptance boundary line (*Bofwd)* to a value exceeding +15.7A, the operation characteristic can be adapted to the transient overcompensation due to post-fault oscillation. However, to ensure dependable and sensitive operation of the protection, *Bofwd* must not be set higher than a value corresponding to the minimum capacitive earth-fault current produced by the background network, considering all practical operation conditions.

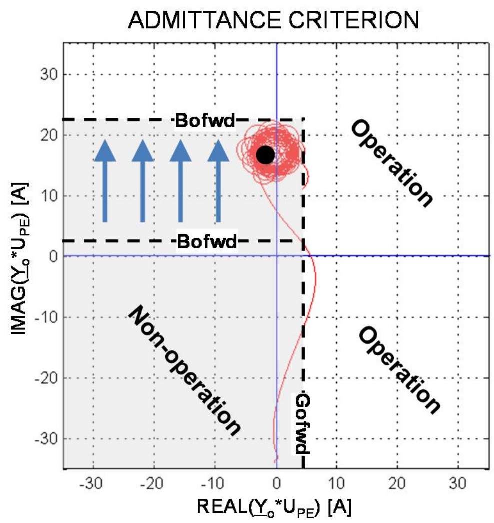

Fig. 7 *Co-ordination of neutral admittance settings for the feeder J05 considering transient overcompensation due to post-fault oscillation.*

Current based directional earth-fault protection

In case residual current based earth-fault protection is applied, operate current, voltage and time settings can be co-ordinated according to duration and amplitude of the post-fault oscillation. The purpose is to select such settings that no false operations occur, while the operating speed and sensitivity requirements of the protection are fulfilled. The residual current of the protected feeder during post-fault oscillation as function of time can be estimated using equation (R_{fault} = *0W*):

$$I_{oP}(t) = |I_{oP}'| \cdot e^{-t/\tau_P} \quad (8)$$

An example setting co-ordination for the feeder *J05* is presented in ***Fig. 8***. A two-stage definite time protection is applied, and the setting selection is based on the estimated time behaviour of the residual current during post-fault oscillation utilizing ***Eq. 8*** (green). Alternatively inverse time protection could be applied. The actual residual current measured in the conducted field tests is plotted as reference (red).

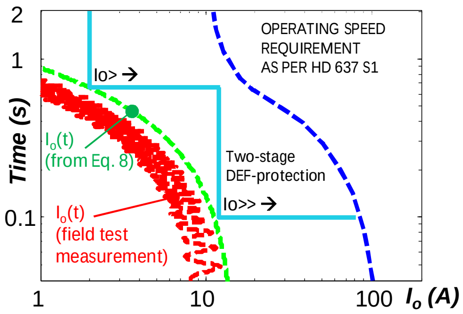

Fig. 8 *Co-ordination of residual current settings for the feeder J05 considering transient overcompensation due to post-fault oscillation.*

If such co-ordination is not feasible, e.g. the requirements set by the legislation cannot be met, simple *current reversal blocking logic* could be used: during an outside fault the residual current is capacitive and flows towards the bus. This activates a dedicated reverse fault indication logic, which blocks the forward looking protection stage. When the residual current turns temporarily to inductive due to post-fault oscillation, the reverse fault indication is kept activated by a drop-off time delay of atleast τ_P. Therefore, the forward looking stage remains blocked during the post-fault oscillation, which prevents false operation. Practical implementation of the logic may require an additional reverse looking stage with a drop-off delay timer to be included into the protection configuration.

POST-FAULT OSCILLATION AND PHASOR CALCULATION

As shown above the risk of transient overcompensation exists for feeders with distributed compensation coils. In practice this means networks with distributed compensation coils where the central coil is not used or it is temporarily disconnected resulting in very low compensation degree. In such networks earth-fault protection is based on the same functionality and settings that are applied in unearthed networks. However, post-fault oscillation also deteriorates the accuracy of phasor calculation, which is experienced especially during intermittent earth faults, where the oscillation repeats itself continuously between fault pulses. This phenomenon is experienced regardless of the applied compensation method, and even with the system compensation degrees close to resonance. The reason for protection maloperation in this case is the decaying magnitude of the oscillation with possible off-nominal (higher or lower) frequency. This is illustrated in ***Fig. 9***, where the behavior of resistive component of residual current (*Iocos*) and admittance (G_o=*Real*($\underline{Y}_o$)) is plotted with different post-fault oscillation frequencies. The time constant of the oscillation is 100ms. Post-fault oscillation is assumed to be initiated after an outside fault and the value of the resistive component is -0.02 per unit during the fault and at the starting instant of the oscillation.

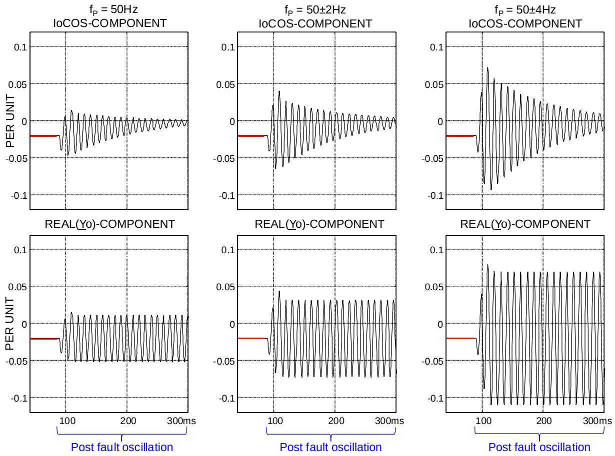

Fig. 9 *Illustration of the fluctuations in the operation quantities of earth-fault protection caused by post-fault oscillation.*

From ***Fig. 9*** it can be seen that already a slight off-nominal frequency together with decaying magnitude of the oscillation causes severe fluctuation in the operating quantities. The greater the frequency deviation is from the nominal, the greater is the fluctuation around the "true" value. As a result, even the sign of resistive component may change, which may lead to unwanted starting (or even operation) of the basic protection in the healthy feeders also during intermittent earth faults.

CONCLUSIONS

This paper described the post-fault oscillation phenomenon, which may lead to transient overcompensation of the protected feeder with distributed compensation coils. The same phenomenon deteriorates the accuracy of phasor calculation during intermittent earth faults, which may lead to unwanted starting or even operation of the basic protection in the healthy feeders. Understanding the theory of this oscillation and its effect on earth-fault protection helps to ensure correct relay operation. Furthermore, protection algorithm design should consider this phenomenon e.g. by means of proper filtering or frequency adaptation.

MISCELLANEOUS

Acknowledgments

This work was supported by Smart Grids and Energy Market research program of CLEEN Ltd, the Strategic centre for science, technology and innovation of the Finnish energy and environment cluster.

REFERENCES

[1] Vehmasvaara S., "*Compensation strategies in cabled rural networks*", Master of Science thesis, 2012

[2] Mäkinen O., 2001, *Intermittent earth fault and relay protection in medium voltage network*, Licentiate thesis, Tampere University of Technology, 107 p. (In Finnish)